

Electronic Supplementary Information (ESI) for New Journal of Chemistry

Tobacco stem-derived nitrogen-containing porous carbon with high dispersed Ni-N sites as an efficient electrocatalyst for CO₂ reduction to CO

Hefang Wang,^{*a} Manhua Li,^a Guanghui Liu,^a Lijia Yang,^a Peidong Sun^a and Shujuan Sun^{*a}

^a School of Chemical Engineering and Technology, Hebei University of Technology, Tianjin 300130, China

E-mail: whf0618@163.com. (Hefang Wang*), sunshujuan@hebut.edu.cn (Shujuan Sun*)

Table of Contents

1. Chemicals
2. Preparation of working electrode
3. Faradaic efficiency (FE) measurements
4. The turnover frequency (TOF) measurements
5. Density Function Theory Calculation
6. Supplemental Figures
7. Supplemental Tables
8. References

1. Chemicals

The tobacco stem used in the experiments was obtained from a Plantation in Shijiazhuang, China. Potassium hydroxide and Nickel (II) acetate tetrahydrate were obtained from Shanghai Macklin Biological Technology. 1,10- Phenanthroline hydrate and Potassium bicarbonate were purchased from Aladdin. Commercial activated carbon, hydrogen peroxide and sulfuric acid were acquired from Tianjin Hengshan Chemical. Nafion solution (5 wt.%) was acquired from Alfa Aesar. All of chemical reagents were of analytical grade and used in the experiment without further purification. Nafion117 membrane was received from DuPont and pretreated via heating in H₂O₂ (5 wt.%) and H₂SO₄ (5 wt.%) at 80 °C for an hour, respectively. Then the Nafion117 membrane was soaked in deionized water for 30 minutes and washed with deionized water several times.

2. Preparation of working electrode

Carbon paper was pretreated by ultrasonication for 30 minutes in ethanol and deionized water, respectively. Typically, 4 mg electrocatalyst was dispersed in 500μL ethanol solution (50 wt.%) and 10μL Nafion solution (5 wt.%), and sonicated for an hour to get a homogeneous catalyst ink. A certain amount of homogeneous ink was dripped onto 1cm×1cm carbon paper (0.8 mg cm⁻² mass loading), which was dried in vacuum oven (60 °C, -0.1 M Pa) for 12 hours.

3. Faradaic efficiency (FE) measurements

The gas products of CO₂ electroreduction were detected by an on-line gas chromatography (GC) (KeChuang GC2002) equipped with a TCD and FID detector. Specifically, H₂ was detected by thermal conductivity detector (TCD) and CO was measured by flame ionization detector (FID). According to detecting concentration of CO or H₂, the FE was calculated by the following equation:

$$FE = \frac{\alpha n F}{Q} \times 100\%$$

α : number of electrons transferred when reduced to the target product (CO or H₂), which is 2;

n : amount of substance of target product;

F : Faraday constant ($F = 96485 \text{ C mol}^{-1}$);

Q : electricity during electrolysis.

4. The turnover frequency (TOF) measurements

According to current density of CO and the Ni loading in the catalyst, the TOF was calculated by the following equation:

$$\text{TOF} = \frac{j_{\text{CO}} M_{\text{Ni}}}{\alpha F m w} \times 3600$$

Where, j_{CO} : current density of CO;

M_{Ni} : atomic mass of Ni, which is 58.69 g mol⁻¹;

α : number of electrons transferred when reduced to CO, which is 2

F: Faraday constant (F = 96485 C mol⁻¹);

m: catalyst mass on the working electrode;

w: Ni loading in the catalyst

5. Density Function Theory Calculation

All geometric optimization calculations are carried out based on the density functional theory (DFT) method as implemented in DMol³ code. Generalized gradient approximation functional with Perdew, Burke and Ernzerhof correlation functional (PBE) is used for the calculation.^{1, 2} The double-numerical basis with polarization functions (DNP) is used with the real-space global orbital cutoff radius set to 4.5 Å and the k-point of the entire Brillouin zone set to 3×3×1 in all computations. The spin-polarized effect is considered in the calculation. During the calculation process, convergence tolerance of energy, maximum force, maximum displacement, and SCF convergence criteria are set to 1 × 10⁻⁵ Ha, 0.002 Ha/Å, 0.005 Å, and of 1 × 10⁻⁶, respectively. In the calculation, a 5×5 and 3×3 supercells are used to construct the graphene and Ni (111) surface structure. And a vacuum region of 18 Å along the z-direction is used to avoid interactions between adjacent images.

Gibbs free energy change of each reaction pathway is defined as $\Delta G = \Delta E + \Delta E_{\text{zpe}} - T\Delta S + \Delta GU$.³ where ΔE is the energy change in each reaction obtained from the density function theory calculations. ΔE_{zpe} and ΔS is change of zero-point energy and entropy for each reaction. And the value of temperature is set as 298.15 K. For the gases molecules, the entropies and vibrational frequencies are taken from the NIST database.⁴ And ΔGU equals to $-neU$ where n is the number of transferred electrons and U is electrode potential applied by external current inputs.

6. Supplemental Figures

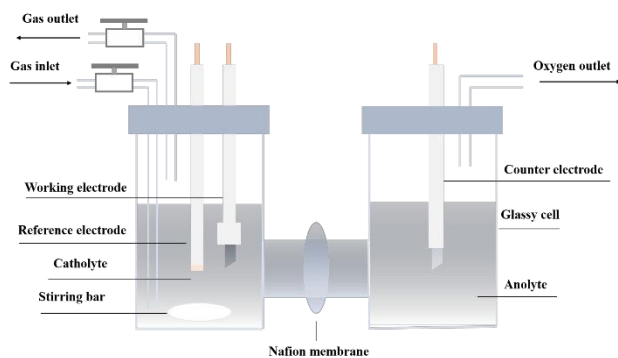


Figure S1. The image of an H-type cell for CO₂ electrolysis.

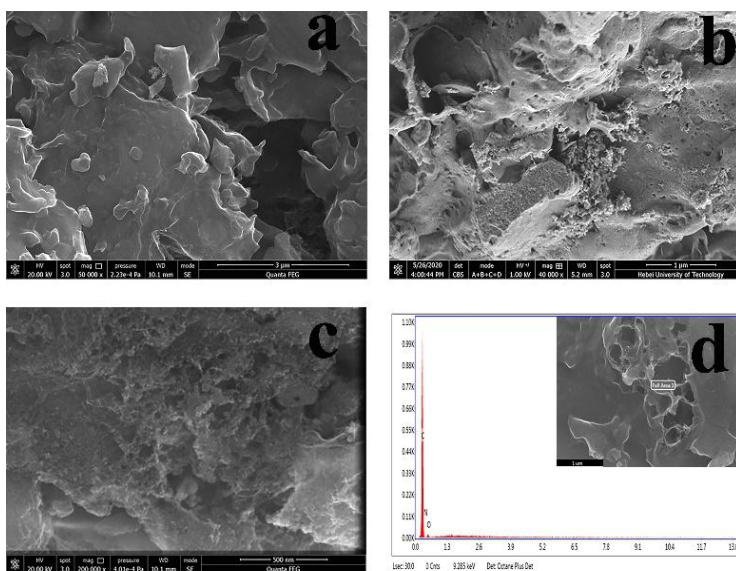


Figure S2. The SEM image of NPC electrocatalyst a) 3 μm b) 1 μm c) 500 nm d) corresponding EDS

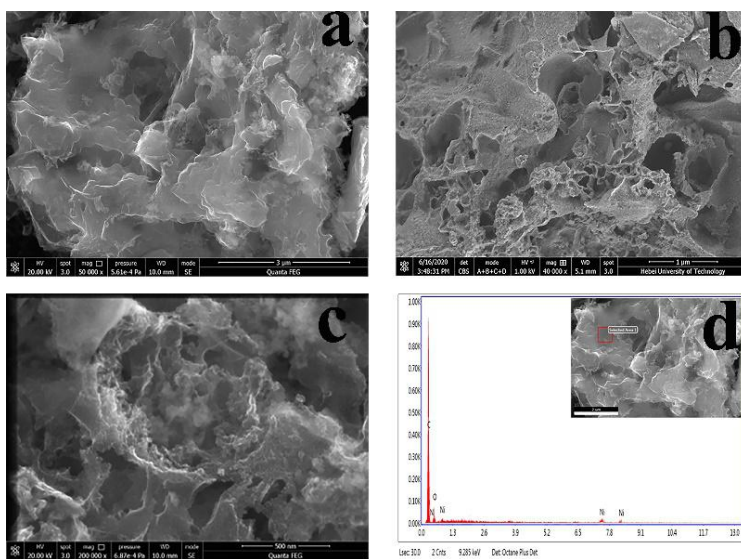


Figure S3. The SEM image of Ni-N@NPC electrocatalyst a) 3 μm b) 1 μm c) 500 nm d) corresponding EDS

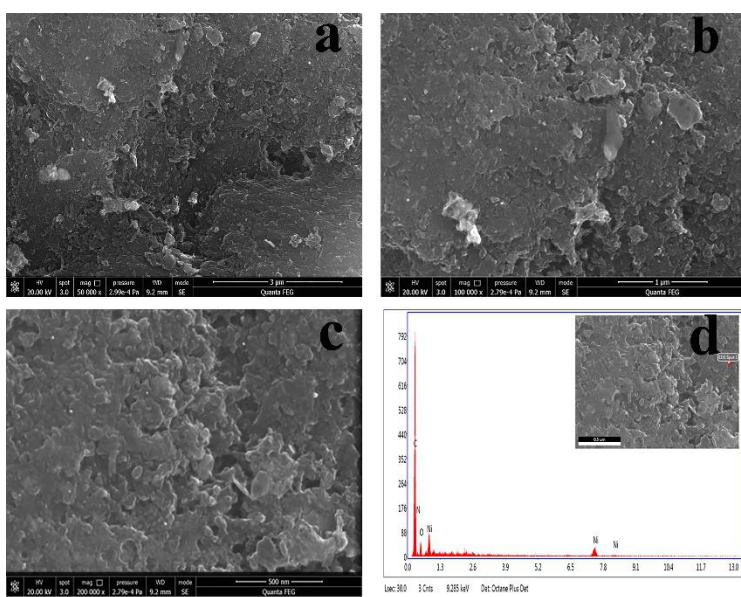


Figure S4. The SEM image of Ni-N@CAC electrocatalyst a) 3 μm b) 1 μm c) 500 nm d) corresponding EDS

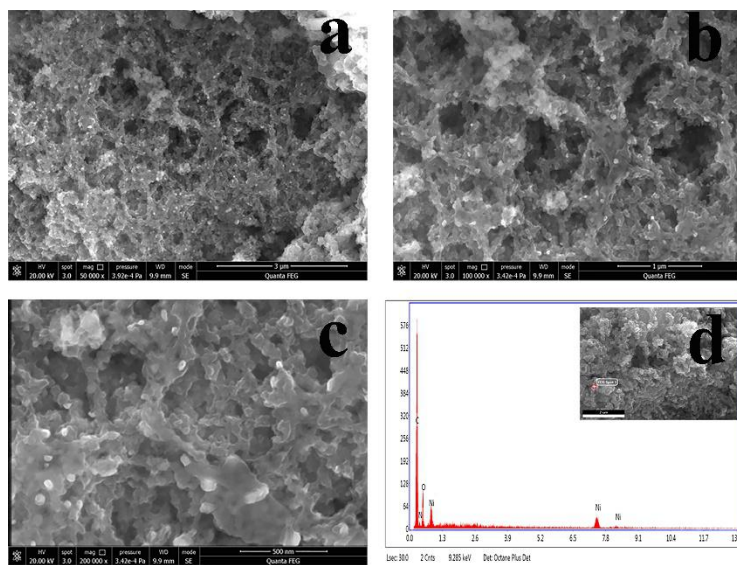


Figure S5. The SEM image of Ni@NPC electrocatalyst a) 3 μm b) 1 μm c) 500 nm d) corresponding EDS

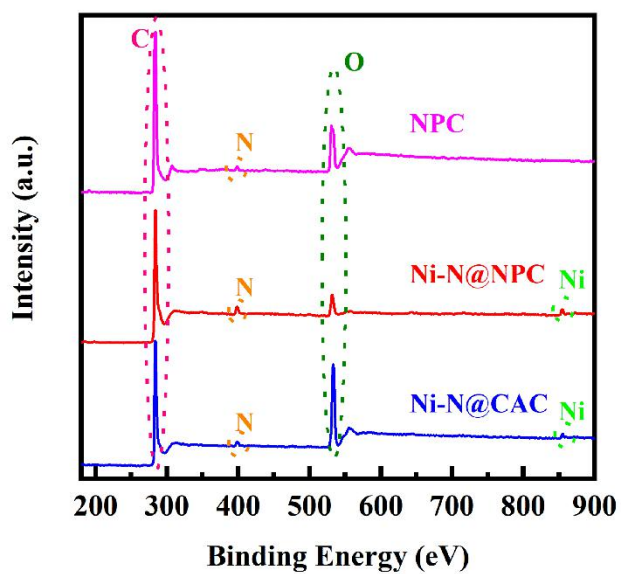


Figure S6. The XPS spectra of NPC, Ni-N@NPC and Ni-N@CAC electrocatalysts.

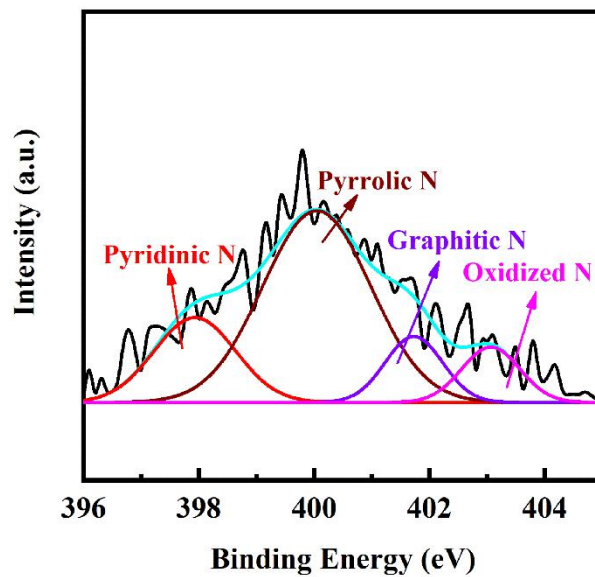


Figure S7. The N 1s spectra of NPC electrocatalyst

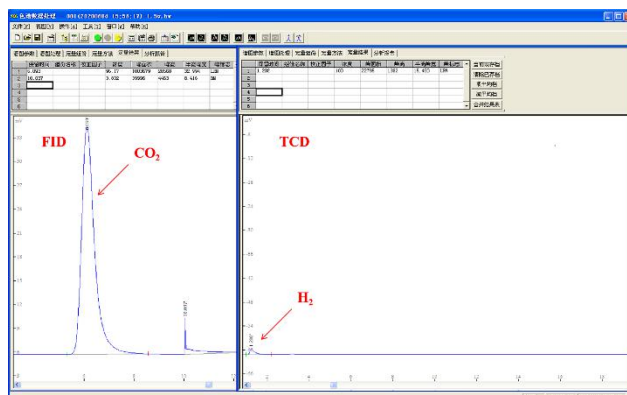


Figure S8. The gas chromatogram of products from Ni-N@NPC electrocatalyst (CO₂ saturated 0.5 M KHCO₃ solution)

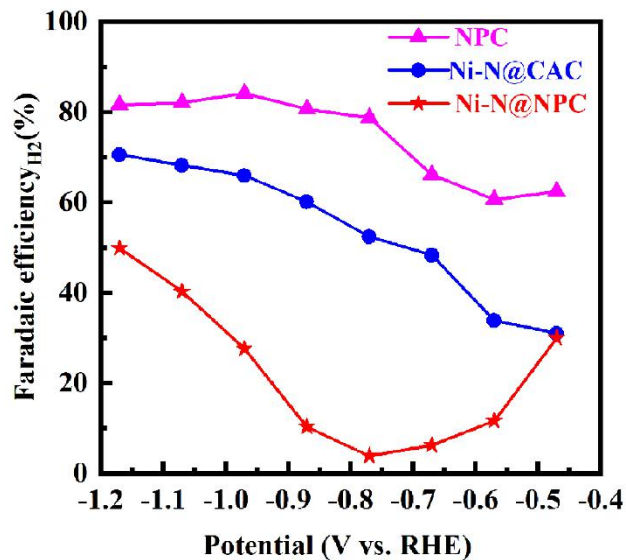


Figure S9. Faradaic efficiency of H₂ for NPC, Ni-N@NPC and Ni-N@CAC electrocatalysts at different potentials

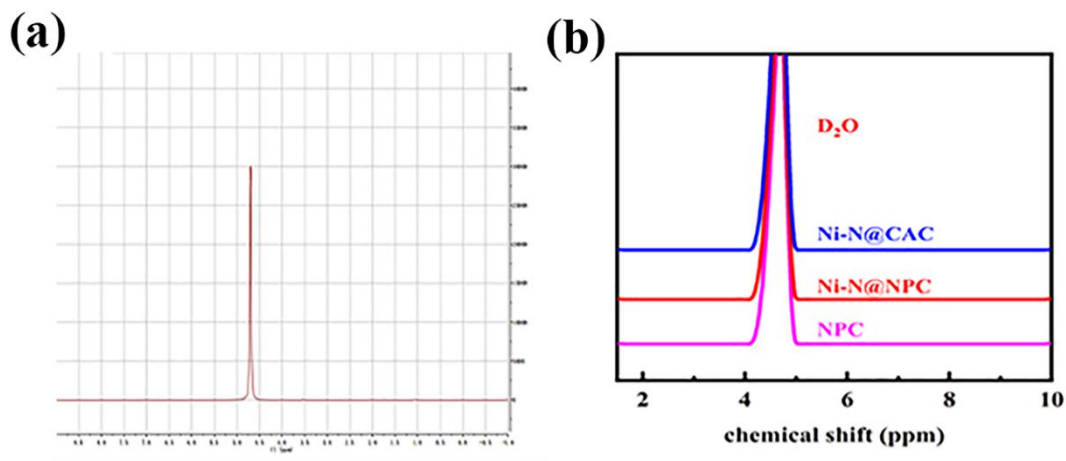


Figure S10. ¹H NMR spectra of the electrolyte after an hour of CO₂ reduction electrolysis for Ni-N@CAC, Ni-N@NPC and NPC electrocatalysts

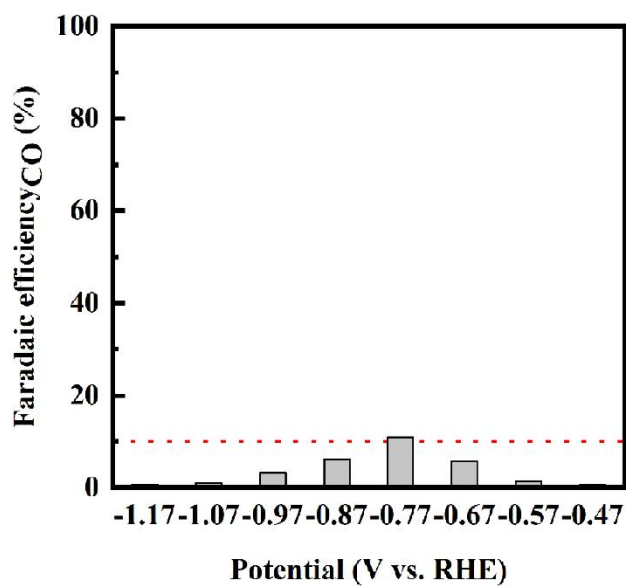


Figure S11. Faradaic efficiency of CO for Ni@NPC electrocatalyst at different potentials

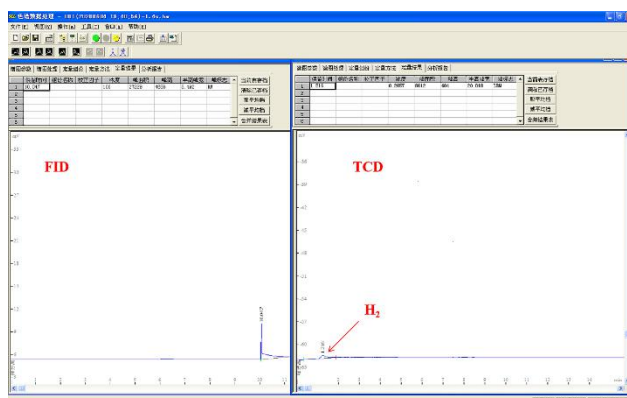


Figure S12. The gas chromatogram of products from Ni-N@NPC electrocatalyst (N₂ saturated 0.5 M KHCO₃ solution)

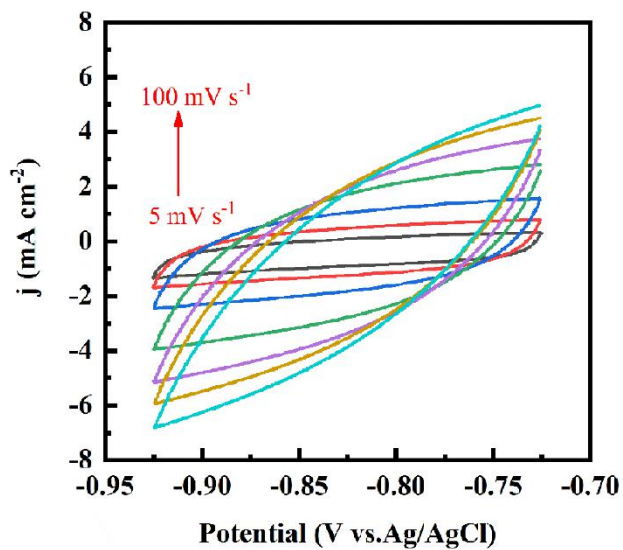


Figure S13. The CVs at the range of -0.73 V to -0.93 V (vs. Ag/AgCl) with difference scan rate (5, 10, 20, 40,60,80,100 mV s^{-1}) for Ni-N@NPC electrocatalyst

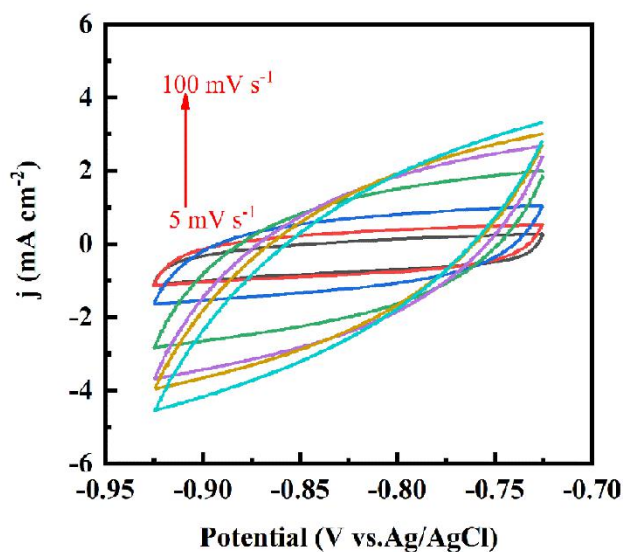


Figure S14. The CVs at the range of -0.73 V to -0.93 V (vs. Ag/AgCl) with difference scan rate (5, 10, 20, 40,60,80,100 mV s^{-1}) for Ni-N@CAC electrocatalyst

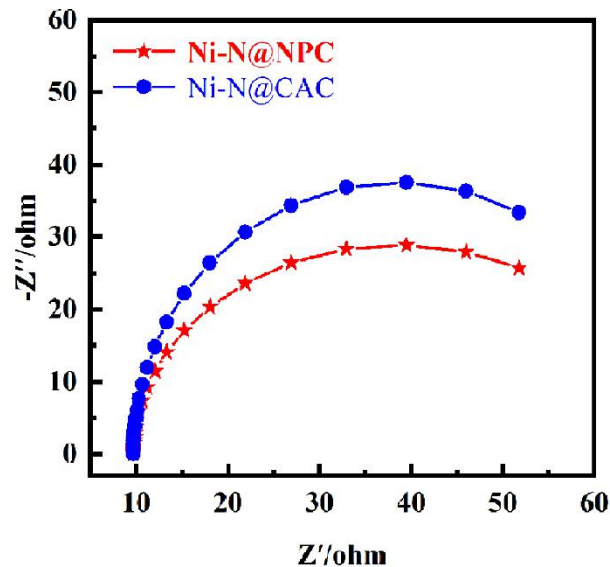


Figure S15. The Nyquist plots for Ni-N@NPC and Ni-N@CAC electrocatalysts

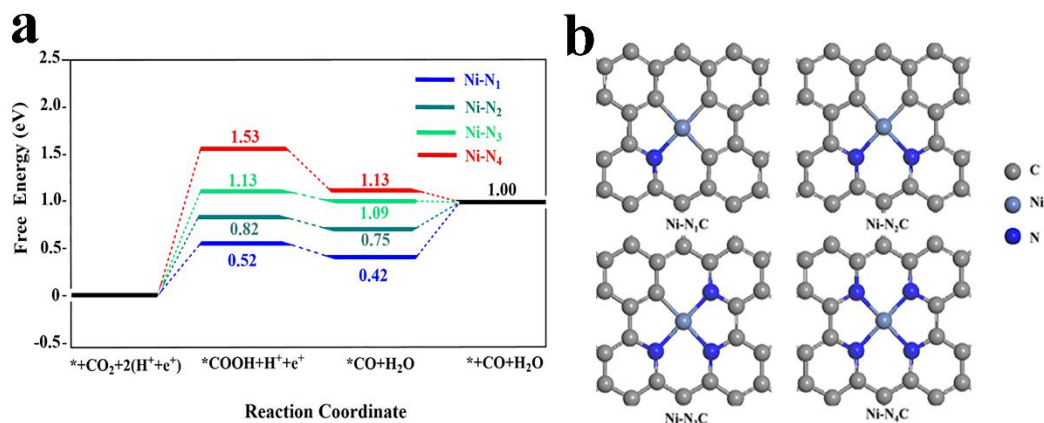


Figure S16. a) The calculation models b) free energy diagrams of Ni-N_x moieties for Ni-N@NPC electrocatalyst

7. Supplemental Tables

Table S1. Textural parameters of the prepared electrocatalysts

Electrocatalysts	S_{BET} ($\text{m}^2 \text{g}^{-1}$)	V_{total} ($\text{cm}^3 \text{g}^{-1}$)	V_{micro} ($\text{cm}^3 \text{g}^{-1}$)	V_{meso} ($\text{cm}^3 \text{g}^{-1}$)	Average pore size (nm)
NPC	2801	1.61	0.15	1.46	3.13
CAC	424	0.45	0.07	0.38	4.26
Ni-N@NPC	1535	1.13	0.11	1.02	3.05
Ni-N@CAC	103	0.07	0.02	0.05	4.10

Table S2. Surface elemental contents and N1s XPS data for Ni-N@NPC, NPC, Ni-N@CAC electrocatalysts

Electrocatalysts	Total C (wt.%)	Total O (wt.%)	Total N (wt.%)	Total Ni (wt.%)	Pyridinic N	Ni-N	Pyrrolic N	Graphitic N	Oxidized N
NPC	57.62	41.15	1.23	-	27.99	-	51.79	10.93	9.29
Ni-N@NPC	53.99	36.67	6.72	2.62	15.12	27.56	35.41	14.67	7.24
Ni-N@CAC	63.20	29.50	4.67	2.63	30.08	18.64	34.70	10.26	6.32

Table S3. Comparison of the activity of Ni-N@NPC with reported electrocatalysts.

Electrocatalysts	Electrolyte	Potential vs. RHE (V)	FE _{CO} (%)	j _{CO} (mA cm ⁻²)	References
Ni-NC SAC	0.5 M KHCO ₃	-0.85	89.00	30.00	5
Fe/NG	0.1 M KHCO ₃	-0.60	80.00	2.70	6
Ni-N-MEGO	0.5 M KHCO ₃	-0.70	92.10	26.80	7
Ni SAs	0.5 M KHCO ₃	-0.80	97.00	10.00	8
Ni-NC@Ni	0.5 M KHCO ₃	-0.77	84.70	14.80	9
ZnCoNC	0.5 M KHCO ₃	-0.55	96.50	71.60	10
Pd-NC	0.5 M NaHCO ₃	-0.50	55.00	2.20	11
Ag/C	0.5 M KHCO ₃	-0.75	84.40	8.00	12
Au (8nm)	0.5 M KHCO ₃	-0.67	90.00	-	13
Au ₃ Cu	0.1 M KHCO ₃	-0.72	64.70	1.80	14
Ni-CTF	0.1 M KHCO ₃	-0.8	90.00	2.5	15
Fe-NC-SBA-15	0.5 M KHCO ₃	-0.47	98.00	-	16
Ni-N@NPC	0.5 M KHCO ₃	-0.77	98.44	30.96	This work

8. References

1. B. Delley, *J. Chem. Phys.*, 1990, **92**, 508-517.
2. B. Delley, *J. Chem. Phys.*, 2000, **113**, 7756-7764.
3. J. R. J. K. Nørskov, A. Logadottir, L. Lindqvist, J. R. Kitchin, T. Bligaard, H. Jónsson, *J. Phys. Chem. B*, 2004, **108**, 17886–17892.
4. C. Ao, B. Feng, S. Qian, L. Wang, W. Zhao, Y. Zhai and L. Zhang, *J. CO₂ Util.*, 2020, **36**, 116-123.

5. L. Zhao, Y. Zhang, L.-B. Huang, X.-Z. Liu, Q.-H. Zhang, C. He, Z.-Y. Wu, L.-J. Zhang, J. Wu, W. Yang, L. Gu, J.-S. Hu and L.-J. Wan, *Nat. Commun.*, 2019, **10**, 1278.
6. C. Zhang, S. Yang, J. Wu, M. Liu, S. Yazdi, M. Ren, J. Sha, J. Zhong, K. Nie, A. S. Jalilov, Z. Li, H. Li, B. I. Yakobson, Q. Wu, E. Ringe, H. Xu, P. M. Ajayan and J. M. Tour, *Adv. Energy Mater.*, 2018, **8**, 1703487.
7. Y. Cheng, S. Zhao, H. Li, S. He, J.-P. Veder, B. Johannessen, J. Xiao, S. Lu, J. Pan, M. F. Chisholm, S.-Z. Yang, C. Liu, J. G. Chen and S. P. Jiang, *Appl. Catal. B: Environ.*, 2019, **243**, 294-303.
8. Z. Li, D. He, X. Yan, S. Dai, S. Younan, Z. Ke, X. Pan, X. Xiao, H. Wu and J. Gu, *Angew. Chem. Int. Ed.*, 2020, DOI: 10.1002/anie.202000318.
9. Y. He, Y. Li, J. Zhang, S. Wang, D. Huang, G. Yang, X. Yi, H. Lin, X. Han, W. Hu, Y. Deng and J. Ye, *Nano Energy*, 2020, **77**, 105010.
10. W. Zhu, L. Zhang, S. Liu, A. Li, X. Yuan, C. Hu, G. Zhang, W. Deng, K. Zang, J. Luo, Y. Zhu, M. Gu, Z. J. Zhao and J. Gong, *Angew. Chem. Int. Ed.*, 2020, **59**, 12664-12668.
11. Q. He, J. H. Lee, D. Liu, Y. Liu, Z. Lin, Z. Xie, S. Hwang, S. Kattel, L. Song and J. G. Chen, *Adv. Funct. Mater.*, 2020, **30**, 2000407.
12. C. Kim, H. S. Jeon, T. Eom, M. S. Jee, H. Kim, C. M. Friend, B. K. Min and Y. J. Hwang, *Journal of the American Chemical Society*, 2015, **137**, 13844-13850.
13. W. Zhu, R. Michalsky, Ö. Metin, H. Lv, S. Guo, C. J. Wright, X. Sun, A. A. Peterson and S. Sun, *J. Am. Chem. Soc.*, 2013, **135**, 16833-16836.
14. D. Kim, J. Resasco, Y. Yu, A. M. Asiri and P. Yang, *Nat. Commun.*, 2014, **5**, 4948.
15. P. Su, K. Iwase, T. Harada, K. Kamiya and S. Nakanishi, *Chem. Sci.*, 2018, **9**, 3941-3947.
16. D. Wu, X. Wang, L. Shi, K. Jiang, M. Wang, C. Lu, Z. Chen, P. Liu, J. Zhang, D. Tranca, Y. Hou, Y. Chen and X. Zhuang, *J. Mater. Chem. A*, 2020, **8**, 21661-21667.